$M_{\alpha\beta}$ X-ray production cross sections of Pb and Bi by 9–40 keV electron impact*

Wu Ying(吴 英)[a)b)†], Wang Guan-Ying(王冠鹰)[a)], Mu Qiang(穆 强)[a)], and Zhao Qiang(赵 强)[a)]

[a)] *School of Nuclear Science and Engineering, North China Electric Power University, Beijing* 102206, *China*

[b)] *Key Laboratory of Radiation Physics and Technology of Ministry of Education, Institute of Nuclear Science and Technology, Sichuan University, Chengdu* 610064, *China*

(Received 8 January 2013; revised manuscript received 4 July 2013; published 12 November 2013)

The experimental data of $M_{\alpha\beta}$ X-ray production cross sections for Pb and Bi by 9–40 keV electron impact have been given. Thin films with thick carbon substrates are used in the experiment. The effects of target structure on the $M_{\alpha\beta}$ X-ray production cross sections are corrected by using the Monte Carlo method. The corrected experimental data are compared with calculated cross sections in terms of the distorted-wave Born approximation (DWBA) theory. The measured $M_{\alpha\beta}$ X-ray production cross sections for Pb and Bi are lower than the DWBA calculations. The atomic relaxation parameters used in comparing the DWBA values with experimental results affect the degree of difference.

Keywords: electron impact, M-shell X-ray production cross sections, Monte Carlo method

PACS: 34.80.Dp, 02.70.Uu **DOI:** 10.1088/1674-1056/23/1/013401

1. Introduction

The study of ionization cross sections of atomic inner shells impacted by keV electrons is significant in both theoretical research and practical applications. It can help us understand the electron–atom interaction and the data of atomic inner-shell ionization cross section by low-energy electron impact have been widely applied in various fields of application.[1–8]

Recently, some models have been proposed through quantum-mechanical calculations for the description of inner-shell ionization by low-energy electron impact, for example, the plane-wave Born approximation theory with Coulomb (C), exchange (Ex), and relativistic corrections (PWBA-C-Ex),[9,10] and the distorted-wave Born approximation theory (DWBA).[3,4] The reliability of calculations needs to be tested by a large number of experimental data. However, experimental data of atomic inner-shell ionization cross sections impacted by low-energy electrons are still scarce.[11–13] For the reported experimental data of K- and L-shell ionization cross sections by electron impact in the incident electron energy region up to several keV, it seems that the DWBA theory is more suitable than the other recently developed theoretical models for the description of atomic ionization.[13–18] Up to now, there are very few studies for M shells.[19,20] In Ref. [19], Merlet *et al.* measured the M_α X-ray production cross sections for Au and Bi by impact of electrons with kinetic energies ranging from the ionization threshold up to 38 keV. Their results have shown that the predictions of the DWBA-EADL are in excellent agreement with their measurements for Au M_α and somewhat overestimate the magnitude of measured values by $\sim 7\%$ for Bi M_α[19] (in the DWBA-EADL calculations, the atomic relaxation parameters that are used to convert the L- and M-subshell ionization cross sections of the DWBA into the M_α X-ray production cross sections are obtained from the evaluated atomic data library (EADL)).[21] In Ref. [20], in the energy range of 3–38 keV, the experimental data of M_α, M_β, and M_γ X-ray production cross sections have been published by Moy *et al.* Their measurements of the M_α X-ray production cross sections are in excellent agreement with the DWBA-EADL cross sections. Their measurements of the M_β line are $\sim 10\%$ larger than DWBA-EADL results, while for the M_γ line, their experimental data are $\sim 20\%$ lower than the DWBA-EADL results. Because there is a large discrepancy among the reported data for some atoms from different groups,[22] to perform a more definite assessment of the reliability of the DWBA for ionization of M shells and check other experimental data, here we measure the $M_{\alpha\beta}$ X-ray production cross sections of Pb and Bi impacted by 9–40 keV electrons. Thin Pb and Bi films deposited respectively onto highly pure thick carbon substrates are used as targets. Our experimental data of $M_{\alpha\beta}$ X-ray production cross sections for Pb and Bi are compared with the DWBA theoretical calculations.

The present paper is organized as follows. The experimental technique and data processing procedure are described in Section 2. In Section 3, we discuss the results. Finally, our conclusions are drawn in Section 4.

*Project supported by the National Natural Science Foundation of China (Grant No. 11275071).

†Corresponding author. E-mail: w_y@ncepu.edu.cn

© 2014 Chinese Physical Society and IOP Publishing Ltd

2. Experiment and data processing

The experimental setup is the same as that we used before,[18,23] so we only give a brief description. The monoenergetic electron beams from 9 keV to 40 keV were provided by an electron gun. The X rays emitted from the targets impacted by keV electrons were detected by an Si (Li) detector with an energy resolution of 170 eV for the ^{55}Mn K_α X ray. The direction of incident electron beam was perpendicular to the direction of Si (Li) detector, and the target was tilted 45° with respect to the direction of the incident electron beam. The current intensity was adjusted in accordance with the X-ray count rates, and the dead time correction was kept at about 1%. The electron beam current was collected by a deep Faraday cup and led to a digital current integrator. The targets used in our experiments were prepared by evaporating elements Pb or Bi on highly pure thick carbon substrates. The targets were made by the China Institute of Atomic Energy. The manufacturer provided the mass thickness values of the target films by weighing. They are 10.5 μg/cm^2 for Pb and 10.7 μg/cm^2 for Bi. A typical X-ray spectrum from the Bi/C target under electron impact is shown in Fig. 1.

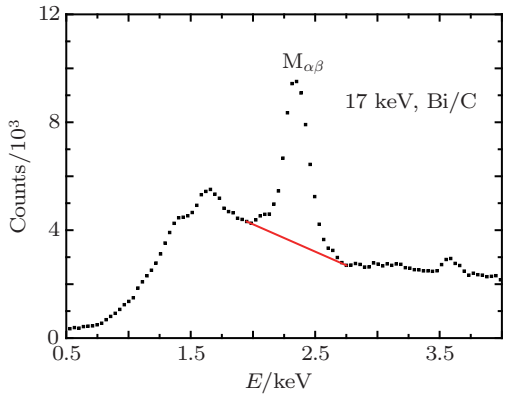


Fig. 1. (color online) Typical characteristic X-ray spectrum for Bi/C target by 17 keV electron impact.

In this work, the homogeneity of the thin targets was examined by recording the beam-induced X rays from different spots of the thin targets. It is estimated to be about 4%. Besides, our group checked the thickness values of the target films for Pb and Bi by using 2 MeV ^{4}He$^+$ Rutherford Backscattering Spectrometry (RBS).[24] They all agree within ∼ 6% with the values given by the target manufacturer. The method of detection efficiency calibration of the Si (Li) detector is identical with that in Ref. [25]. The shape of the efficiency calibration curve was determined from the ratio of the experimental to the theoretical bremsstrahlung spectra of thick-target carbon by electron impact, and the absolute values of the efficiency calibration were obtained by using the ^{241}Am standard radioactive source. The theoretical bremsstrahlung spectrum of thick-target carbon by 19 keV electron impact was calculated by using the Monte Carlo code PENELOPE.[26] The uncertainty in the detection efficiency calibration by this method mainly comes from the standard radioactive sources and is estimated to be ∼ 5%.[25]

The method of data processing is similar to that used earlier for measuring the L-shell X-ray production cross sections of Pb and Bi.[18,23] Although the target films are very thin, incident electrons do undergo some scattering and lose energy within the film. Therefore, the effective path length of electrons is larger than the film thickness and the effective energy is slightly smaller than the energy of incidence. Furthermore, part of electrons backscattered from the thick substrate and bremsstrahlung photons produced by incident electrons bombarding the target may also lead to ionization of target atoms while passing through the target film. These effects will contribute to the counts of the characteristic X-ray peaks. We denote this contribution to the counts as ΔN. If we define a K factor as the ratio of ΔN to N (N is the net count of the characteristic X-ray peak), the X-ray production cross section can be obtained by

$$\sigma(E_e) = \frac{4\pi A(1-K(E_e))}{N_A t N_e \varepsilon(E_{ph})\Omega} N(E_e), \quad (1)$$

where σ denotes the X-ray production cross section, E_e is the incident electron energy, A is the atomic weight, E_{ph} is the produced photon energy, N_A is the Avogadro constant, t is the thin film mass thickness, N_e is the number of incident electrons, $\varepsilon(E_{ph})$ and Ω are the intrinsic efficiency and the solid angle subtended by the detector system, respectively.

The K factors were obtained by Monte Carlo simulations with the PENELOPE-2005 code.[26] The $M_{\alpha\beta}$ X-ray production cross sections by electron impact with the corresponding characteristic X-ray counts $N_{M\alpha\beta,MC}$ from the X-ray spectrum generated by Monte Carlo simulation with PENELOPE can be given by

$$\sigma_{M_{\alpha\beta},MC} = \frac{2A}{N_e N_A t} N_{M_{\alpha\beta},MC}, \quad (2)$$

where A, N_e, N_A, and t are defined in Eq. (1). In addition, the inner-shell ionization cross sections and other atomic parameters (e.g., fluorescence yields, Coster–Kronig transition probabilities, X-ray emission rates, and radiative plus nonradiative transition yields) used in the Monte Carlo simulations can be obtained from the database of the PENELOPE code[26] and converted into $M_{\alpha\beta}$ X-ray production cross sections using the following equation:

$$\begin{aligned}\sigma_{M_{\alpha\beta}} = {} & \frac{\Gamma_{M_5N_{6,7}}}{\Gamma_{M_5-Total}}\omega_{M_5}[\sigma_{M_1}(f_{15}+f_{14}f_{45}+f_{13}f_{34}f_{45}+f_{13}f_{35} \\ & +f_{12}f_{23}f_{34}f_{45}+f_{12}f_{25}+f_{12}f_{23}f_{35}+f_{12}f_{24}f_{45}) \\ & +\sigma_{M_2}(f_{25}+f_{24}f_{45}+f_{23}f_{34}f_{45}+f_{23}f_{35}) \\ & +\sigma_{M_3}(f_{35}+f_{34}f_{45})+\sigma_{M_4}f_{45}+\sigma_{M_5} \\ & +\sigma_{L_3}\eta_{L_3M_5}+\sigma_{L_2}\eta_{L_2M_5}+\sigma_{L_{11}}\eta_{L_1M_5}]\end{aligned}$$

$$+\frac{\Gamma_{M_4N_6}}{\Gamma_{M_4-\mathrm{Total}}}\omega_{M_4}[\sigma_{M_1}(f_{14}+f_{13}f_{34}+f_{12}f_{24}+f_{12}f_{23}f_{34})+\sigma_{M_2}(f_{24}+f_{23}f_{34})+\sigma_{M_3}f_{34}+\sigma_{M_4}+\sigma_{L_3}\eta_{L_3M_4}+\sigma_{L_2}\eta_{L_2M_4}+\sigma_{L_1}\eta_{L_1M_4}], \quad (3)$$

where σ_{L_i} and σ_{M_i} are the cross sections for the ionization of the L_i and M_i subshells, respectively; ω_{M_i} is the M_i subshell fluorescence yield; f_{ij} are the Coster–Kronig transition probabilities between the M_i and M_j subshells; $\Gamma_{M_iN_{j,k}}$ and Γ_{M_i} are the fractional and total X-ray emission rates for M_i shell; $\eta_{L_1M_i}$, $\eta_{L_2M_i}$ and $\eta_{L_3M_i}$ are the radiative plus nonradiative yeilds for transitions of vacancies from the L_1, L_2 and L_3 subshells to the M_i subshell. The latter parameters were only used if the incident electron energy is larger than the L-shell ionization threshold.

Finally, the K factors can be obtained by

$$K=\frac{\sigma_{MC}-\sigma_{th}}{\sigma_{MC}}. \quad (4)$$

After the K factors are obtained, we can obtain the $M_{\alpha\beta}$ X-ray production cross sections using Eq. (1). The final experimental results are summarized in Table 1. The experimental uncertainties mainly come from the statistical uncertainties of measured peaks (which are about 2%–5% for Pb–$M_{\alpha\beta}$ and 2%–7% for Bi–$M_{\alpha\beta}$), detection efficiency ($\sim$ 5%),[26] target thickness ($\sim$ 6%), number of incident electrons ($\sim$ 1%), K factors ($\sim$ 3%),[28] and inhomogenity of the target ($\sim$ 4%). Therefore, the total uncertainties of $M_{\alpha\beta}$ X-ray production cross sections obtained by quadratic addition are estimated to be $\sim$ 12% for Pb, and $\sim$ 12%–14% for Bi.

Table 1. $M_{\alpha\beta}$ X-ray production cross sections of Pb and Bi by electron impact measured in the present paper.

E_e/keV	X-ray production cross section/barn	
	Pb $M_{\alpha\beta}$	Bi $M_{\alpha\beta}$
9	823	851
10	846	859
11	813	859
12		834
13	807	852
14		848
15		838
16	801	825
17	762	811
19	716	802
20	712	773
21	706	760
22	714	751
23	693	
24		763
25	684	
26		728
27	662	
28		686
29	651	
30		664
31	649	
32		616
33	625	
34		593
35	591	
36		613
37	581	
38		
39	551	
40	535	581

3. Results and discussion

Figures 2 and 3 show the present experimental data of $M_{\alpha\beta}$ X-ray production cross sections for Pb and Bi in comparison with the DWBA theory.[3,4,28] The atomic parameters, which are adopted in the conversion of the DWBA L- and M-subshell cross sections[3,4,28] into $M_{\alpha\beta}$ X-ray production cross sections based on Eq. (3), are listed in Tables 2, 3, and 4. In order to observe the effects of atomic parameters on the calculations of M-shell X-ray production cross sections, in this work we use two sets of different relaxation parameters. One set of atomic parameters are all taken from the results calculated by Puri *et al.*,[29,30,34] namely, the M-subshell fluorescence yields, the Coster–Kronig transition probabilities are taken from Ref. [29], and the radiative plus nonradiative yields for

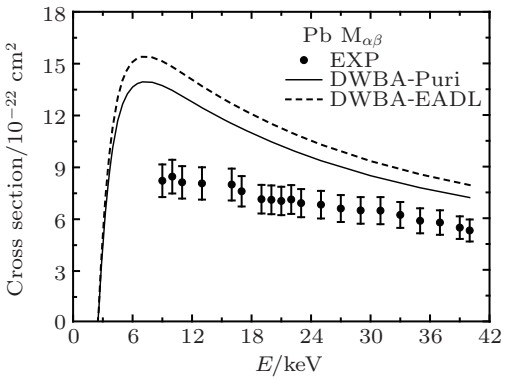


Fig. 2. Pb $M_{\alpha\beta}$ X-ray production cross sections versus incident electron energy. The solid circles indicate the present experimental data. The solid line and dash line represent the DWBA theoretical result combined with relaxation data extracted from the values reported by Puri *et al.*[29,30,34] and the EADL,[21] respectively.

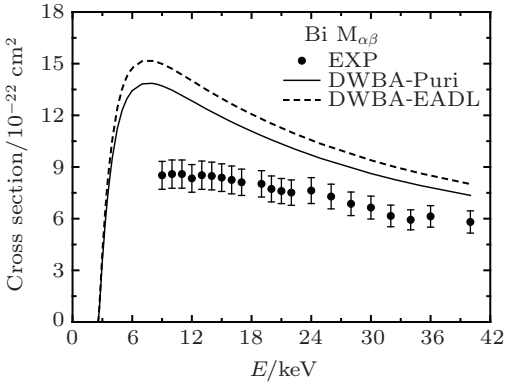


Fig. 3. Bi $M_{\alpha\beta}$ X-ray production cross sections versus incident electron energy. The solid circles indicate the $M_{\alpha\beta}$ present experimental data. The solid line and dash line represent the $M_{\alpha\beta}$ DWBA theoretical result combined with relaxation data extracted from the values reported by Puri *et al.*[29,30,34] and the EADL,[21] respectively.

vacancies from the L_i subshell to the M_i subshell are obtained from Ref. [30]. Because the atomic parameters combined with the radiative transition probabilities computed from the Dirac–Fock (DF) model were found to be more reliable than those computed using the Dirac–Hartree–Slater (DHS) model,[31–33] in this paper the atomic parameters given by Puri *et al.*[29,30,34] are based on the DF model except for the Coster–Kronig yields, which are based on the DHS model. In addition, the second set of atomic parameters which are all taken from the EADL[18] are also used.

Table 2. M_i-subshell fluorescence yields for Pb and Bi elements adopted in this work.[29] X-ray emission rates for Pb and Bi elements taken from Ref. [34] in this work.

	ω_{M_1}	ω_{M_2}	ω_{M_3}	ω_{M_4}	ω_{M_5}	$\Gamma_{M_5N_{6,7}}/\Gamma_{M_{5-Total}}$	$\Gamma_{M_4N_6}/\Gamma_{M_{4-Total}}$
Pb	0.00317	0.00485	0.00671	0.03251	0.03096	0.9297	0.9403
Bi	0.0034	0.00523	0.00715	0.03392	0.03233	0.9584	0.9431

Table 3. M_i-subshell Coster–Kronig transition probabilities for Pb and Bi elements adopted in this work.[29]

	f45	f12	f13	f14	f15	f23	f24	f25	f34	f35
Pb	0.054	0.121	0.592	0.0892	0.123	0.105	0.682	0.109	0.066	0.735
Bi	0.057	0.117	0.594	0.0898	0.123	0.106	0.679	0.11	0.067	0.738

Table 4. Radiative plus nonradiative probabilities for transitions of vacancies from the L subshells to M_i subshell adopted in this work.[30]

	$\eta_{L_1M_5}$	$\eta_{L_2M_5}$	$\eta_{L_3M_5}$	$\eta_{L_1M_4}$	$\eta_{L_2M_4}$	$\eta_{L_3M_4}$	$\eta_{L_1M_3}$	$\eta_{L_2M_3}$
Pb	0.874	0.258	0.687	0.487	0.59	0.247	0.291	0.141
Bi	0.863	0.250	0.684	0.482	0.591	0.243	0.287	0.137
	$\eta_{L_3M_3}$	$\eta_{L_1M_2}$	$\eta_{L_2M_2}$	$\eta_{L_3M_2}$	$\eta_{L_1M_1}$	$\eta_{L_2M_1}$	$\eta_{L_3M_1}$	
Pb	0.318	0.107	0.237	0.061	0.119	0.047	0.049	
Bi	0.313	0.108	0.233	0.06	0.120	0.047	0.049	

It is seen from Figs. 2 and 3 that in the whole enery region of interest, the DWBA-EADL values are $\sim 10\%$ larger (for Pb $M_{\alpha\beta}$) and $\sim 9\%$ larger (for Bi $M_{\alpha\beta}$) than the DWBA-Puri results, and our experimental data of $M_{\alpha\beta}$ X-ray production cross sections for Pb and Bi impacted by 15–40 keV electron are about 20%–30% smaller than the DWBA–Puri calculations. Whereas in the electron energy range of 9–15 keV, our measured data for Pb and Bi are about 30%–40% smaller than the DWBA-Puri values. This point is different from the experimental results of Merlet *et al.* for Bi[19] and Moy *et al.* for Pb.[20] In Refs. [19] and [20], the DWBA calculations were combined with atomic parameters taken from the EADL[21] and were $\sim 7\%$ larger than the experimental data for Bi M_α, in good consistence with the experimental data for Pb M_α, and somewhat lower than the experimental data for Pb M_β. The atomic parameters adopted from different references for calculating the M-shell X-ray production cross sections can affect the degree of difference between the DWBA theory and the experimental data. To observe the influence degree, we compute the DWBA cross sections for Bi M_α combined with atomic parameters from the results calculated by Puri *et al.*[29,30,34] Figure 4 shows that the predictions of the DWBA-EADL are about 9%–14% higher than the corresponding DWBA-Puri values in the electron energy range of 3–40 keV. The experimental results of Merlet *et al.*[19] are all in agreement with the DWBA-Puri values.

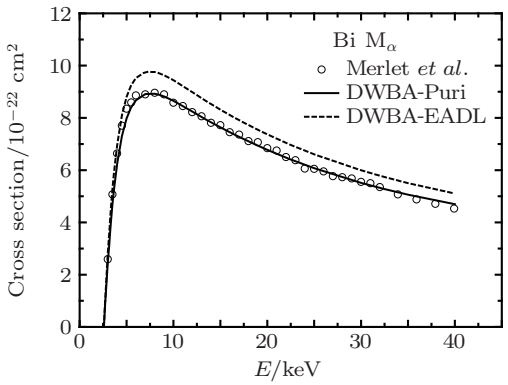


Fig. 4. Bi M_α X-ray production cross sections versus incident electron energy. The open circles denote the M_α experimental data of Merlet *et al.*[19] The solid line indicates the M_α DWBA theoretical result combined with the EADL[21] and the dash line denotes the M_α DWBA theoretical result combined with Puri *et al.*[29,30,34]

As mentioned above, the atomic relaxation parameters adopted from different authors can lead to a difference in the theoretical results compared with the experimental data. Moreover, our experimental data of $M_{\alpha\beta}$ X-ray production cross sections for Pb and Bi are smaller than the DWBA-Puri calculations. It is different from other experiments. For example, the experimental results of Merlet *et al.* for Bi M_α[19] are in consistence with the DWBA-Puri values. Although some similar conclusions that the experimental values of atomic

inner-shell cross sections are much lower than the DWBA calculated values have been given,[16,35,36] we still need to pay attention to this difference prudently. Even though we have taken into account all possible factors, more accurate measurements of M-shell X-ray production cross sections for high-Z elements by keV electrons impact need be done.

4. Conclusions

In summary, we have performed measurements of $M_{\alpha\beta}$ X-ray production cross sections for elements Pb and Bi by 9–40 keV electron impact. The experimental data are compared with the DWBA calculations. The results show that our corrected experimental values of $M_{\alpha\beta}$ X-ray production cross sections for Pb and Bi are lower than the DWBA calculations. Besides, the atomic relaxation parameters usually affected by sizable uncertainties are used in comparing theoretical results with the experimental data.

Acknowledgments

We would like to thank Prof. Z. An, Dr. Y. M. Duan and associate professor M. T. Liu for their help during the experiment. We also thank the staff of the electrostatic accelerator in Institute of Nuclear Science and Technology of Sichuan University for their help during the RBS experiments.

References

[1] Powell C J 1976 *Rev. Mod. Phys.* **48** 33
[2] Powell C J 1985 in *Electron Impact Ionization* (Ed. T. D. Märk and G. H. Dunn) (New York: Springer-Verlag) pp. 198–231
[3] Nagashima Y, Saito F, Itoh Y, Goto A and Hyodo T 2004 *Phys. Rev. Lett.* **92** 223201
[4] Segui S, Dingfelder M and Salvat F 2003 *Phys. Rev. A* **67** 062710
[5] Colgan J, Fontes C J and Zhang H L 2006 *Phys. Rev. A* **73** 062711
[6] Salzmann D, Reich Ch, Uschmann I, Förster E and Gibbon P 2002 *Phys. Rev. E* **65** 036402
[7] Riley D, Angulo-Gareta J J, Khattak F Y, Lamb M J, Foster P S, Divall E J, Hooker C J, Langley A J, Clarke R J and Neely D 2005 *Phys. Rev. E* **71** 016406
[8] Köster P, Akli K, Batani D, Baton S, Evans R G, Giulietti A, Giulietti D, Gizzi L A, Green J S, Koenig M, Labate L, Morace A, Norreys P, Perez F, Waugh J, Woolsey N and Lancaster K L 2009 *Plasma Phys. Contr. Fusion* **51** 014007
[9] Hippler R 1990 *Phys. Lett. A* **144** 81
[10] Khare S P and Wadehra J M 1996 *Can. J. Phys.* **74** 376
[11] Wu Z W, Yang D L, Luo X B, He F Q, Peng X F and Luo Z M 2003 *Chin. Phys. Lett.* **20** 1485
[12] Gou C J, Wu Z W, Peng X F, He F Q and Luo Z M 2005 *Chin. Phys. Lett.* **22** 2538
[13] Wu Y, An Z, Duan Y M, Liu M T and Ouyang X P 2012 *Can. J. Phys.* **90** 125
[14] Zhu J J, An Z, Liu M T and Tian L X 2009 *Phys. Rev. A* **79** 052710
[15] Wu Y, An Z, Duan Y M and Liu M T 2010 *Nucl. Instrum. Methods Phys. Res. B* **268** 2820
[16] Wu Y, An Z, Duan Y M, Liu M T and Wu J 2011 *Nucl. Instrum. Methods Phys. Res. B* **269** 117
[17] Wu Y, An Z, Duan Y M and Liu M T 2010 *J. Phys. B* **43** 135206
[18] Wu Y, An Z, Duan Y M and Liu M T 2010 *Nucl. Instrum. Methods Phys. Res. B* **268** 2473
[19] Merlet C, Llovet X and Salvat F 2008 *Phys. Rev. A* **78** 022704
[20] Moy A, Merlet C, Llovet X and Dugne O 2013 *J. Phys. B* **46** 115202
[21] Perkins S T, Cullen D E, Chen M H, Hubbell J H, Rath J and Scofield J 1991 *Report UCRL*-50400 30 (Livermore, CA: Lawrence Livermore National Laboratory)
[22] Llovet X, Merlet C and Salvat F 2000 *J. Phys. B* **33** 3761
[23] Wu Y, An Z, Duan Y M, Liu M T and Tang C H 2007 *J. Phys. B* **40** 735
[24] An Z, Liu M T, Fu Y C, Luo Z M, Tang C H, Li C M, Zhang B H and Tang Y J 2003 *Nucl. Instrum. Methods Phys. Res. B* **207** 268
[25] An Z and Liu M T 2002 *Nucl. Instrum. Methods Phys. Res. B* **194** 513
[26] Salvat F, Fernández-Varea J M and Sempau J 2005 *PENELOPE*: *A Code System for Monte Carlo Simulation of Electron and Photon Transport*
[27] Wu Y and An Z 2006 *Nucl. Phys. Rev.* **23** 62 (in Chinese)
[28] Bote D, Salvat F, Jablonski A and Powell C J 2009 *At. Data Nucl. Data Tables* **95** 871
[29] Chanhan Y and Puri S 2008 *Atomic Data and Nuclear Tables* **94** 38
[30] Chauhan Y, Kumar A and Puri S 2009 *Atomic Data and Nuclear Tables* **95** 475
[31] Khan M R and Karimi M 1980 *X-ray Spectrom* **9** 32
[32] Papp T, Campbell J L and Raman S 1993 *J. Phys. B* **26** 4007
[33] Puri S, Mehta D, Singh N and Trehan P N 1996 *Phys. Rev. A* **54** 617
[34] Puri S 2007 *Atomic Data and Nuclear Tables* **93** 730
[35] Campos C S, Vasconcellos M A Z, Llovet X and Salvat F 2002 *Phys. Rev. A* **66** 012719
[36] Shevelko V P, Solomon A M and Vukstich V S 1991 *Phys. Scr.* **43** 158